Synthesis and Characterization of Sulfonated Poly(arylene sulfone) Terpolymers with Triphenylphosphine Oxide Moieties for Proton Exchange Membrane Fuel Cells

G. Titvinidze[1]*, A. Kaltbeitzel[1], A. Manhart[1], W. H. Meyer[1]*

[1] Max Planck Institute for Polymer Research, Ackermannweg 10, Mainz 55128, Germany

[*] Corresponding Authors, meyer@mpip-mainz.mpg.de, titvini@mpip-mainz.mpg.de

Abstract

For application in fuel cells, a series of sulfonated poly(phenylene sulfone) terpolymers with triphenylphosphine oxide moieties as constitutional units in the polymer backbone have been prepared. The synthesis of the terpolymers represents a two-step process including: 1) an aromatic nucleophilic substitution polycondensation of three difluoro monomers with varying ratios, *i.e.* 3,3'-disulfonate-4,4'-difluorodiphenylsulfone, 4,4'-difluorodiphenylsulfone and bis(4-fluorophenyl)phenyl phosphine oxide (BFPPO), with 4,4'-thiobisbenzenethiol yielding sulfonated poly(phenylene sulfide) terpolymers (sPPSPO) and 2) their following oxidation with hydrogen peroxide in acidic solution to yield sulfonated poly(phenylene sulfone) terpolymers (sPPSO2PO). The structures and molecular compositions were confirmed by ^{1}H and ^{13}C NMR spectroscopy. The ion exchange capacity (IEC) was adjusted at will choosing the appropriate ratio of sulfonated and unsulfonated monomers. Terpolymers with $1{,}72 \leq IEC \leq 2{,}32$ have been obtained. Sulfonated poly(arylene) ionomers containing only sulfone ($-SO_2-$) linkages and phosphine oxide (-PO-) units rather than ether or sulphide in the backbone reveal a high thermal and oxidative stability. Membranes were cast either from DMF or from DMSO solutions. For all terpolymers some general characteristic trends were observed, such as an increase of the proton conductivity with increasing IEC, water uptake and temperature. The series of sPPSO2PO membranes offered high conductivities at high humidification, however, their performance strongly depends on the relative humidity.

The mechanical properties of sulfonated poly(phenylene sulfone)s have been considerably improved by means of terpolymerization with phenylene oxide moieties. Even under high humidification the terpolymers form clear, flexible membranes the stress at break of some membranes exceeds that of Nafion® under the same conditions by 40%.

Keywords: Fuel Cells, Sulfonated Poly(phenylene sulfone) Terpolymers, Ionomer Membranes, Proton Conductivity.

1 Introduction

Power supply relying on electrochemical processes is a promising alternative to combustion engines. In this respect, polymer electrolyte membrane fuel cells (PEMFC) seem to be very promising, environmentally friendly power converters, which can be used for automotive applications, as well as for stationary and mobile applications. PEMs are the key components in the fuel cells [1-3]. Perfluorinated sulfonic acid membranes such as Nafion® are used nowadays in commercial fuel cells, but they have severe drawbacks, namely cost and environmental issues and limitation of the operation temperature to below 100°C. In addition, Nafion and other

perfluorinated sulfonic acid membranes suffer from low conductivity at low water contents or high temperatures, relatively low mechanical strength at higher temperature, low stability at high temperatures, and high methanol crossover [4-6]. To overcome these drawbacks, in recent years a number of alternative membranes have been developed [2-11].

Among the alternative materials investigated, sulfonated aromatic polymers, such as sulfonated poly(arylene sulfone)s [12-15], poly(arylene ether ketone)s [16-20], sulfonated poly(arylene ether sulfone)s [8,21-25], polyimides [26-29], sulfonated poly(benzimidazole)s [30-33], have been proposed as alternative materials for PEMFCs. They show high proton conductivity, excellent thermal and oxidative stability, good mechanical properties, good processability, exceptional hydrolytic stability and relatively low cost. These sulfonated aromatic polymers can be prepared either by post-sulfonation of the aromatic polymers or by direct copolymerization of the sulfonated monomer. As compared to the post-sulfonation, the direct copolymerization allows to control the degree of sulfonation and decreases the possibility of side reactions that may occur during the post-sulfonation process [34-42].

Sulfonated (p-phenylene sulfone) (sPSO2) polymers are among the most promising materials for PEMFC applications. They were synthesized *via* a two-step polymerisation described by Schuster *et al*. [12]. sPSO2s show high conductivities, good mechanical properties and higher hydrolytic stability in comparison with poly(arylene ether sulfone)s and poly(arylene sulfide sulfone)s and much lower methanol crossover as compared to Nafion®. High hydrolytic stability is caused by electron-withdrawing groups like sulfone (-SO2-), ketone (-CO-), or phosphine oxide (-PO-) in the *ortho*- and *para*-position to the sulfonic acid group. This is very important for their application under harsh conditions prevailing in a fuel cell (T > 100°C in acidic, high humidity environment) [12].

Phosphine oxide fragments containing sulfonated aromatic polymers are showing challenging properties [43-45]. Introduction of phosphine oxide fragments in the polymer backbone enhances mechanical properties, oxidative stability, water retention and adhesion to inorganic materials [46-48]. Since the polymer chain of polysulfones usually are highly symmetrical, thus leading to brittleness and low solubility, the introduction of unsymmetrical groups disrupting this arrangement seems to be an interesting way to improve the mechanical properties and solubility.

For this reason an approach of terpolymerization of sulfonated and unsulfonated monomers for the control of the ion exchange capacity (IEC) was combined with the introduction of symmetry breaking triphenylphosphine oxide moieties (BFPPO) to synthesize terpolymers and characterize their properties in view of their application as membranes for fuel cells.

2 Experimental Part

2.1. Materials

3,3'-disulfonate-4,4'-difluorodiphenylsulfone (K), 4,4'-difluorodiphenylsulfone (L) and 4,4'-thiobisbenzenethiol (N) were purchased from FuMA-Tech GmbH (Germany). 4,4'-thiobisbenzenethiol was purified by further recrystallization from ethanol. Bis(4-fluorophenyl)phenyl phosphine oxide (BFPPO, M) (97%, Aldrich), anhydrous potassium carbonate (99%, Acros Organics), calcium carbonate (99%, Aldrich), N-methyl-2-Pyrrolidone (NMP) (99,5%, extra dry over molecular sieve, water <50 ppm, Acros Organics), dimethylformamide (DMF) (99,8%, Aldrich), dimethyl sulfoxide (DMSO) (99,9%, Aldrich) and toluene (99,8%, Aldrich) were used without further purification.

2.2 Synthesis of Polymers

Sulfonated poly(phenylene sulfide) as precursor terpolymers with triphenylphosphine oxide moieties in the backbone (sPPSPO) were synthesized *via* nucleophilic substitution polycondensation reactions of K, L M and N. In the following the synthesis of sPPSO2PO-3 (s. Table 1, scheme 1) will be explicitly shown, exemplifying the procedure described by Schuster *et al* [12].

3,3'-disulfonate-4,4'-difluorodiphenylsulfone (2.000 g, 4.37 mmol), 4,4'-difluorodiphenylsulfone (0.158 g, 0.62 mmol), BFPPO (0.392 g 1.25 mmol), 4,4'-thiobisbenzenethiol (1.560 g, 6.24 mmol) and K_2CO_3 were placed in a round-bottom flask equipped with a magnetic stirrer, an argon inlet/outlet and Dean-Stark trap with a condenser. Then, NMP (5 mL) and toluene (5 mL) were charged into the reaction flask under nitrogen atmosphere. The mixture was heated up to 150°C and kept refluxing for 4 h to remove the water by azeotropic distillation. Afterwards the excess of toluene was removed by emptying the Dean-Stark trap and the mixture was heated to 180°C for 48 h to complete the polycondensation. After the reaction had completed, the resulting dark purple solution was cooled to room temperature and diluted with 5 ml DMF. Subsequently, the polymer was precipitated from 2-propanol (80 ml). In order to remove all by- and low-molecular products, the polymer was purified by dialysis for 72 h (dialysis tubing cellulose ester membrane, 2 000 MWCO, Spectra/Por Biotech). After removal of water by freeze drying a yield of 3.591 g (93 %) was calculated. ^{1}H NMR (250 MHz, DMSO-d_6): δ=8.25 (H_a), 7.96 (H_b), 7.84 (H_c, H_d, H_e), 7.66 (H_f), 7.58-7-47 (H_g, H_h, H_i, H_j), 7.36 (H_k), 6.93 (H_l). ^{13}C NMR (62.9 MHz, DMSO-d_6): δ=173.93 (s), 144.54 (s), 144.12 (s), 138.37 (s), 136.50 (s), 136.15 (s), 135.90 (s), 134.62 (s), 133.81 (s), 132.27 (s), 132.09 (s), 131.99 (s), 131.89 (s), 131.85 (s), 130.70 (s), 130.07 (s), 128.22 (s), 128.13 (s), 127.71 (s), 127.59 (s), 126.03 (s), 126.00 (s).

The poly(phenylene sulfide) terpolymer precursor sPPSPO-3 was oxidized following the same procedure as described by Schuster *et al*. [12]: 3.499 g sodium-form sPPSPO-3 was suspended in a 10:1 mixture of 80 ml glacial acetic acid (Aldrich) and concentrated sulphuric acid (95-97%, Aldrich). Subsequently 6 ml hydrogen peroxide (35% H_2O_2 in water, Aldrich) was dropwise added and the mixture was stirred for 48 hours at 35°C. The reaction mixture was heated up to 100°C to remove the excess of peroxide. The product was separated by filtration and washed several times by deionized water, which was further removed by freeze drying yielding 3.752 g (97%) sPPSO2PO-3. ^{1}H NMR (250 MHz, DMSO-d_6): δ=8.60 (H_a), 8.56 (H_b), 8.27 (H_c), 8.21 (H_d), 8.06 (H_e), 7.99 (H_f), 7.92-7.84 (H_h, H_i, H_j), 7.65 (H_k), 7.58 (H_l). ^{13}C NMR (62.9 MHz, DMSO-d_6): δ=162.31 (s), 149.23 (s), 146.34 (s), 146.16 (s), 144.91 (s), 144.42 (s), 143.94 (s), 143.38 (s), 142.93 (s), 140.46 (s), 133.51 (s), 133.21 (s), 133.04 (s), 129.48 (s), 129.14 (s), 128.07 (s), 127.90 (s).

Terpolymers sPPSO2PO-4 and sPPSO2PO-5 were synthesized according to the same procedure, while terpolymers sPPSO2PO-1 and sPPSO2PO-2 were obtained by direct oxidation of membranes sPPSPO-1 and sPPSPO-2. In order to remove all by- and low-molecular products, the terpolymers sPPSO2PO-4 and sPPSO2PO-5 were purified by ultrafiltration with deionized water (100 000 NMWL**,** Millipore Co.) instead of using dialysis.

All spectral data of the terpolymers are very similar to the one presented in Figure 1.

2.3 Membrane Preparation

Membranes of the terpolymers were prepared in two different ways: i) Terpolymers sPPSPO-1 and sPPSPO-2 were dissolved in DMF (10 wt %), filtered with 5 μm filter, cast onto dust free glass plates (Petri dishes) and dried at 50°C in vacuum for 48 hours. Membranes were pilled off from the plates by soaking in deionized water, dried in vacuum at 50°C for 12 hours. Eventually they were oxidized according to the above described procedure. ii) Terpolymers sPPSO2PO-3, sPPSO2PO-4 and sPPSO2PO-5 were dissolved in DMSO (2.5-5 wt %), cast onto dust free glass plates and dried at 60^0C in vacuum for 72 hours. After film formation, the membranes were pilled off from the plates by immersing in 10% H_2SO_4 solution. sPPSPOs were transformed to the acid form by proton exchange in 10% H_2SO_4 solution for 24 hours at 80^0C. Afterwards, the membranes were washed several times with deionized water and stored in it. Membranes prepared according to the second route were transparent, while in the ones prepared according to the first way transparency was not reached.

2.4 Characterization of Terpolymers

^{1}H and ^{13}C NMR spectra were recorded using Bruker Spectrospin 250 and Bruker DSX500 spectrometers at room temperature with deuterated dimethyl sulfoxide (DMSO-d_6) as a solvent and internal standard.

Molecular weight measurements were done by gel permeation chromatography (GPC) using a Waters 515 system equipped with three consecutive Polymer Standards Service columns (GRAM, 10 000, 1 000, 100) calibrated by standard polystyrene (Polymer Standard Service), UV detector (Soma S-3702) and RI detector (ERC 7512; ERMA). The GPC measurements were performed in DMF at 60^0C at a flow rate of 1.0 mL min^{-1}.

Thermogravimetric Analysis (TGA) was carried out on a TGA/SDTA-851 (Mettler-Toledo) under nitrogen at a heating rate of 10 K min^{-1} and T_{d5} was reported as temperature at which 5% weight loss was observed. Before analysis, the films were dried in vacuum at 50°C for at least 24 h to remove absorbed water. Differential scanning calorimetry (DSC) was carried out on a Mettler-Toledo DSC-30 under nitrogen at a heating rate of 10 K min^{-1}.

2.5 Proton Conductivity Measurements

Proton conductivity results were derived from dielectric spectroscopy in a two-electrode geometry using an SI 1260 impedance/gain-phase analyzer and a Novocontrol broadband dielectric converter. Proton conductivities under different humidification (different degree of hydration) were measured in a temperature controlled climate chamber (Binder KBF 240) with a working humidity range between 18 and 95% of relative humidity (RH). Membranes were equilibrated in the climate chamber at the specified RH and temperature for at least 10h before measurement. An atmosphere of saturated humidity was generated by using a closed sample cell with a water reservoir on the bottom that was not in contact with the sample. Saturation was controlled by a Sensirion SHT75 humidity sensor and found to be 100% (within the error bar of the sensor (2%)). From Cole-Cole and Bode plots, the specific conductivity of the composite membrane was estimated. Conductivity was measured in through plane as well as in plane geometry. For the in plane measurements membranes of size 10 x 15mm were fixed between two E-tek^R electrodes, for through plane measurements stacks of 8-16 membranes were placed between E-tek^R electrodes and pressed by screws to ensure maximum contact.

Conductivity measurements in pure H_2O-atmosphere ($p(H_2O) = 10^5$ Pa) above 100°C were carried out in a double wall temperature controlled glass oven with a gas inlet and outlet. To constantly flush the sample with a pure H_2O-atmosphere, water was evaporated, the gas subsequently adjusted to the desired temperature and piped through the heated inlet of the glass oven. A pressure of 10^5 Pa adapts itself due to the small outlet of the oven

against ambient. The atmosphere set by this equipment is comparable to a fuel cell under operation, where water is formed at the cathode. It should be noted that the relative humidity, set by a H_2O-atmosphere at 10^5 Pa, decreases with increasing temperature according to the table of vapor pressure. For example, 10^5 Pa water vapor pressure at 120°C corresponds to a relative humidity of ~ 50% (*i.e.* $2 \cdot 10^5$ Pa = 2 bar are needed for condensation), at 150°C the same water pressure corresponds to a RH close to 20% only.

2.6 Water Uptake and Shrinkage Ratio

The water uptake (WU) and the shrinkage ratio (SR) were obtained by measuring the differences in the weight and length under different humidification. Prior to the measurements the films were thoroughly dried at 100°C for 24 hours and subsequently stored at an atmosphere of fixed relative humidity (RH) until a constant weight was obtained. Different relative humidities were adjusted using different salt solutions [49]. Typically, the water uptake equilibrated within 36-48 h. The WU was calculated according to Eq. (1):

$$\mathrm{WU}\,(\%) = \frac{W_{rh} - W_{dry}}{W_{dry}} \times 100 \qquad (1)$$

where W_{rh} is the weight of the membrane at a specific relative humidity and W_{dry} is the weight in the dry state. The hydration number λ was calculated on the basis of WU as the number of water molecules per sulfonic acid unit.

The procedure for the determination of the shrinkage ratio SR is similar to the WU measurements. It was calculated according to Eq. (2):

$$\mathrm{SR}\,(\%) = \frac{l_{wet} - l_{rh}}{l_{wet}} \times 100 \qquad (2)$$

where l_{wet} is the length of a membrane stored in water and l_{rh} is the length of the membrane at a specific humidification. Together with the length the thickness changes were measured in the same way.

2.7. Oxidative stability

The xidative stability was investigated by soaking a thoroughly dried membrane sample (10 x 10 x 0.15 mm) with precise weight in Fenton's reagent (30% H_2O_2 containig 30 ppm $FeSO_4$) at 25°C. The stability was evaluated by recording the weight loss with time.

2.8 Mechanical Strength

Tensile tests were carried out using the Instron Universal Testing Machine (Model 6022) equipped with a 100 N load cell. Stress strain curves were obtained at a speed of 1.0 mm min^{-1} for dogbone specimens sized 4 x 20mm. The sample was embedded in a chamber in which the relative humidity was adjusted by mixing dry and humidified nitrogen.

2.9. Atomic force microscopy (AFM)

Tapping mode AFM observations were performed by Dimension 3100 Atomic Force Microscope, using Olympus tapping mode cantilevers OMCL-AC160TS-W2 with a force constant of 42 N/m and resonance frequency of around 300 kHz. All images were taken under ambient conditions (RH ≈ 50%).

3 Results and discussion

3.1 Synthesis

Sulfonated PPSPOs precursor polymers with different compositions and ion exchange capacities (IEC) were successfully synthesized *via* nucleophilic aromatic substitution polycondensation reactions using the three difluoro monomers BFPPO, 3,3'-disulfonate-4,4'-difluorodiphenylsulfone and 4,4'-difluorodiphenylsulfone to react with 4,4'-thiobisbenzenethiol in different molecular ratios (s. Table 1).

At first the aprotic dipolar reaction system was dehydrated by azeotropic distillation using toluene. Dehydration is very important to obtain high yields and thus high molecular weights. The reactions proceeded for 48 h in order to obtain completely converted products. After precipitation of polymers from 2-propanol, they were purified by dialysis/ultrafiltration or in the case of the water-insoluble polymers by washing with deionized water. All synthesized precursor polymers are soluble in common polar aprotic solvents, such as NMP, DMF, DMSO and DMAc. The solubility of the precursors depends on the sulfonation degree and increases with increasing IEC.

As fuel cell membranes are exposed to harsh conditions (T>100°C in high humidity environment, possible formation of $HO^{\cdot}$ or $HO_2^{\cdot}$ radicals at the cathode or anode [50]), oxidative and hydrolytic stability plays an important role. Polymers having sulfide (-S-) or ether (–O-) groups in the main chain are less stable than polymers with electron-withdrawing sulfone groups (-SO_2-) [12] and their application in fuel cells is problematic. To increase the oxidative and hydrolytic stability PPSPOs were oxidized to PPSO2POs according

to the procedure described by Schuster *et al* [12]. The solubility decreases when going from PPSPOs to PPSO2POs. Therefore the membranes were obtained by two different ways: Since sPPSO2PO-1 and sPPSO2PO-2 were insoluble in common casting solvents films were obtained by casting the precursors sPPSPO-1 and sPPSPO-2 from 10% DMF solution. The membranes were subsequently oxidized. In case of sPPSO2PO-3, sPPSO2PO-4 and sPPSO2PO-5 the solubility was sufficient to directly cast the corresponding sPPSO2POs from DMSO solution. Membranes obtained according the first route are not transparent, probably because of incomplete oxidation. Several attempts to optimize the oxidation conditions to get full oxidation of the films were not successful. Membranes cast according to the second way are transparent. Independent from the preparation procedure all membranes are flexible in their water-swollen form and become more or less brittle in the dry state, depending on their composition. The general two-step synthetic route for the terpolymers is shown in Scheme 1.

The structures and compositions of sPPSPOs and sPPSO2POs were confirmed by ^{1}H and ^{13}C NMR spectroscopy. The ^{1}H NMR spectra of sPPSPO-3 and its corresponding oxidized form sPPSO2PO-3 are shown in Figure 1 as an example to assign the signals given in the experimental part. As evident from Figure 1 all signals coincide with the proposed structure of the terpolymers. The integration of ^{1}H NMR spectra was in good accordance with the ones expected from the feed monomer ratio. Furthermore, using ^{13}C NMR the spectra also confirmed the structure of the terpolymers.

The GPC analysis shows that high molecular weight terpolymers were obtained. As expected, high molecular weights improve the film forming properties and the mechanical properties of the terpolymers in their dry and water swollen state. The IEC (mequiv g^{-1}) values, number and weight average molecular weights (M_n and M_w) and polydispersity indices of the synthesized polymers are summarized in Table 1. In all cases the yields were higher than 90%.

3.2 Thermal Properties

The thermal stability of the synthesized terpolymers was evaluated by thermogravimetric analyses (TG) (Figure 2). The membranes (acid form) were analyzed in the temperature range 30-600°C under dry nitrogen flow. For all samples a three-step weight loss was observed. The first loss from 30 to 175°C can be assigned to the loss of adsorbed water, the second loss at 320-420^{0}C was presumably due to desulfonation and the third one above 420^{0}C was attributed to the degradation of the polymer backbone. The 5% (w/w) loss temperature (T_{d5}) data for the terpolymers are summarized in Table 1. There is no correlation with IEC or other parameters. Sulfonated PPSO2PO terpolymers are thermally stable systems with decomposition temperatures (T_d) above 300°C under

nitrogen. Differential scanning calorimetry (DSC) did not show any glass transition temperature below the decomposition temperature (T_d). This can be explained by the significant broadening of the temperature range of the glass transition which is typical for ionomers having high ion content [51].

3.3 Water Uptake and Swelling Ratio

The water uptake (WU) of sulfonated membranes plays an important role in proton conductivity as water acts as transport medium of protons; it also has a strong impact on the mechanical properties [52]. High water uptake leads to higher conductivities, but on the other hand causes critical dimensional changes and reduces the mechanical stability of the membranes. Therefore, a balanced WU is necessary for the application as PEMs. The water uptake was measured as a function of RH at 25°C as described in the experimental part. In Figure 3 the WU data are provided in weight percent. As expected, the WU increases with increasing IEC due to the introduction of strongly hydrophilic sulfonic acid groups. According to the water uptake values of sPPSPO-5 and sPPSO$_2$PO-5 it is evident that the precursor terpolymers (sPPSPO) have higher water uptake than corresponding poly(phenylene sulfone) terpolymers (sPPSO2PO). In Table 2 the λ values are presented, which are defined as the number of water molecules per sulfonic acid unit at a water activity of 1. There is a significant deviation of λ values obtained from samples immersed in water as compared to those that were stored at 100% RH despite the fact that in both cases the chemical activity of water is 1. The WU of samples in contact with liquid water exceeded those from samples at saturated water vapor by a factor of 1.5-2.0. This phenomenon is known as the Schroeder's paradox and several explanations are reported on the basis of different WU kinetics [53-58]. However, since the data reported in Table 2 have been obtained after "equilibration" of the samples, i.e. after waiting unless no weight change could be observed anymore, it remains a paradox in this case .

The dimensional changes of the membranes sPPSO2PO-3, sPPSO2PO-4 and sPPSO2PO-5 were investigated as described in the experimental part. In Table 2 the dimensional changes of the terpolymer films are shown. Since the thickness d and length l data are initially determined in the fully swollen state, and the membranes are exposed to 52,4%, 34% and 20% RH, the dimensional changes are negative due to a shrinkage of the membranes. The anisotropy of the proton conductivities for in plane and through plane measurements which are discussed in the next chapter can be explained by anisotropic swelling. From the data it is evident that the shrinkage prevails in the humidity range from 100% to 50%, below 50% RH the shrinkage remains less than the error bar.

3.4 Proton Conductivity

The proton conductivities for series of sPPSO2PO terpolymers were measured as function of relative humidity in the range of 100≤RH≤20% at 25°C, as function of temperature at 80% RH and as function of temperature above 100°C (100-160°C) under one bar of water vapour atmosphere. For an appropriate evaluation of the results, it was decided to compare the conductivities of Nafion® as reference, however, measured with the same technique rather than citing literature data. The proton conductivity as a function of RH is shown in Figure 4. As expected, the proton conductivity increases with increasing RH, which corresponds to increasing hydration according to Figure 3. However, the conductivity decreases more rapidly at low RH as compared to Nafion®. In Figure 4 are included the data for through plane measurements of the membranes sPPSO2PO-1 and sPPSO2PO-5. In both cases the through plane proton conductivities are higher as compared to in plane data. It was supposed that this difference is caused by anisotropic swelling and/or an unsymmetrical microstructure. The strong dependence of the proton conductivity on hydration is not surprising. It was already suggested in the literature that at low hydration levels the connectivity between sulfonic acid groups, which is necessary for proton transport, decreases [11, 59, 60].

For random terpolymers, a higher IEC is required to reach comparable conductivities to that of perfluorinated sulfonic acid ionomers such as Nafion®. This is due to the nanoscale phase separation of the ionic and non-ionic domains in the ionomers and a higher local acidity of the perfluorosulfonic acid groups in the hydrophilic domains. For random terpolymers, the proton conductivity usually follows the IEC. In Figure 5 there are compared the proton conductivity data at high hydration levels (95% RH) as a function of IEC. With the exception of sPPSO2PO-1, the proton conductivities of the sPPSO2PO membranes increase almost linearly with the IEC. Only the sample sPPSO2PO-1 has surprisingly low proton conductivity as compared to PPSO2PO-2 despite their similar ion exchange capacities (1,74 and 1,72 mequiv g^{-1}). It was assumed that this might be due to a different microstructure developed during film formation. The lower phosphine oxide content of sPPSO2PO-1 might also have an impact on the water retention properties. The decrease of the proton conductivity going from sPPSO2PO-4 with lower IEC=2,01 mequiv g^{-1} to sPPSO2PO-5 with higher IEC=2,19 mequiv g^{-1} is within the error bar. From the data it can be concluded that there is a strong correlation between water uptake and IEC (correlation factor c=0.99) and a lower but still significant correlation between conductivity and IEC (c=0.86). The decrease in correlation can be explained by the fact that morphology plays a crucial role for conductivity and that adsorbed water does not contribute effectively to the proton conduction.

The temperature dependence of the proton conductivities for the series of the sPPSO2PO terpolymers at RH=80% is shown in Figure 6. Each point was obtained after equilibrating the sample until the conductivity was

constant within the error bar. These data show that the proton conductivities increase with increasing temperatures. This might be explained by both, a typical thermal activation of the proton transport, and by an effective increase of the hydration number with increasing temperature. From Figure 6 apparent activation energy values were evaluated. For Nafion, the calculated value (10.3 kJ/mol) is in good agreement with Springer et al. [61] (10.5kJ/mol). Due to nonlinear behaviour below 35°C, data evaluation was limited to the temperature range between 35°C and 85°C. With the exception of sPPSO2PO-1, the activation energies of the membranes are slightly higher as compared to Nafion, lying in a range between 10.7 and 12.5 kJ/mol. For sPPSO2PO-1 a value of 4.7 kJ/mol was calculated. It was assumed that due to incomplete oxidation (see above) domains with variable conductivity form beneath the surface. These domains are subject of changes upon heating leading to less reliable data for the calculation of the activation energy.

It should also be kept in mind, that data from Fig. 6 only reflect an apparent activation energy. Activation energy for transport processes is usually thought as the height of a potential barrier against the freedom of flow in a quasi lattice structure. However, such a lattice does not exist in the membranes investigated. Especially for Nafion it is known, that charge carriers rather flow in channels of liquid water. Therefore, well-defined activation barriers are also not involved in Nafion [62].

For fuel cell membranes one of the key parameters is the dependence of proton conductivity on relative humidity. In Figure 7 are presented the proton conductivity data of the terpolymers at 1 bar water vapor for the membranes sPPSO2PO-2, sPPSO2PO-4 and sPPSO2PO-5. At each temperature 1 bar water pressure corresponds to a certain value of RH (160°C ≈16% RH, 150°C ≈ 20%, 143°C ≈ 25% RH, 120°C ≈ 50% [63]). Terpolymer sPPSO2PO-4 and sPPSO2PO-5 show conductivity values which are comparable to Nafion® at high RH and sPPSO2PO-5 even exceeds the proton conductivity of the Nafion® 117 around 100°C, however, at low RH the conductivities are significantly lower.

For all the membranes obtained from the terpolymers some general trends were observed, such as an increase of the proton conductivity with increasing water uptake, temperature and IEC. The performance of the random terpolymers strongly depends on the relative humidity and their conductivities are still unsatisfying at low humidification.

3.4. Oxidative stability

The oxidative stability was investigated by Fenton's test for terpolymers sPPSO2PO-1, sPPSO2PO-3, sPPSO2PO-5 and sPPSPO-5 as described in the experimental part. Figure 8 summarizes the stability data for the membranes. For all sPPSO2PO membranes there was no change in membrane integrity observable even after 30 hours, while a weight loss could already be observed (Figure 8). After 60 hours the sPPSO2PO membranes also lost its integrity, while the sPPSPO precursor membrane lost its integrity already after 20 hours. From the comparison of the oxidative stability data of sPPSPO-5 and sPPSO$_2$PO-5 it is evident that the poly(phenylene sulfone) terpolymers are more stable than the corresponding poly(phenylene sulfide)s. The oxidative stability of the sulfonated poly(phenylene sulfone) terpolymers containing triphenylphosphine oxide moieties is almost independent from IEC, similar to the poly(phenylene sulfone)s described by Schuster *et al*. [12]. These results indicate the concept of improving the stability of membranes via introduction of electron-withdrawing groups proves successful.

3.5 Mechanical Properties

In order to guarantee the integrity of the membrane under fuel cell operating conditions, PEMs need an excellent mechanical strength to cope with the high mechanical stresses appearing in a fuel cell [64]. The mechanical strength of the membranes was evaluated in a tensile test at 25°C at 50% RH (which is close to the humidity during fuel cell operation) and at 100% RH. Stress-strain curves are displayed in Figure 9 and the values of stress at break, elongation at break and Young's modulus are summarized in Table 2. Comparing the curves of sPPSO2PO-5 under 50% and 100% RH, it is evident that water acts as plasticizer and weakens the intermolecular interactions leading to an increase of elongation at break and deterioration of the mechanical stability [2]. In Fig. 9 the correlation of the mechanical strength with IEC was checked by comparing sPPSO2PO-3 to -5. Increasing the IEC from 2.01 up to 2.32 equiv g^{-1} the value of elongation at break increases from 15.1 to 19.8 % at 50% RH, The sample sPPSO2PO-5 exhibits the highest stress at break. Generally, the stress at break values of the membranes are in the same range as that of Nafion®, nevertheless sPPSO2PO-5 shows an almost 40% higher stress at break. In Figure 9 the values fore a sulfonated poly(phenylene sulfone) (sPPSO2-X, without PO-units) with IEC=2.34 equiv g^{-1} are included, which can be compared with sPPSO2PO-5 (IEC = 2.32 equiv g^{-1}) as they have almost the same IEC. From Figure 9 it is evident that the mechanical properties are superior in the material containg phosphine oxide moieties.

3.6. Morphology

Morphology investigations for sPPSO2PO membranes were performed by AFM. Tapping mode phase images were recorded under ambient conditions on a 500 nm X 500 nm size scale. However, no phase contrast could be observed which can be attributed other than surface roughness of the films, which depends on the film preparation. Obviously, the introduction of triphenylphosphine oxide moieties apparently does not lead to phase separated systems. The microstructures of the materials are still under SAXS investigations and will be reported in a separate publication.

4 Conclusions

A series of sulfonated poly(phenylene sulfone) terpolymers with triphenylphosphine oxide moieties as constitutional units in the polymerbackbone have been prepared. The synthesis of the terpolymers represents a two-step process including: i) an aromatic nucleophilic substitution polycondensation of three difluoro monomers with varying ratios, *i.e.* 3,3'-disulfonate-4,4'-difluorodiphenylsulfone, 4,4'-difluorodiphenylsulfone and bis(4-fluorophenyl)phenyl phosphine oxide (BFPPO), with 4,4'-thiobisbenzenethiol yielding sulfonated poly(phenylene sulfide) terpolymers (sPPSPO) and ii) their following oxidation with hydrogen peroxide in acidic solution to yield sulfonated poly(phenylene sulfone) terpolymers with triphenylphosphine oxide moieties (sPPSO2PO). Since there are no indications for preferred reactivities a random distribution of the monomer units in the terpolymers is assumed. The ion exchange capacity (IEC) was adjusted at will choosing the appropriate ratio of sulfonated and unsulfonated monomers. Terpolymers with $1{,}72 \leq IEC \leq 2{,}32$ have been obtained. Sulfonated poly(arylene) ionomers containing only sulfone ($-SO_2-$) linkages and phosphine oxide (-PO-) units rather than ether or sulphide in the backbone reveal a high thermal and oxidative stability. Membranes were cast either from DMF or from DMSO solutions. For all terpolymers some general characteristic trends were observed, such as an increase of the proton conductivity with increasing IEC, water uptake and temperature. The series of sPPSO2PO membranes offered high conductivities at high humidification, however, their performance strongly depends on the relative humidity. At low humidities the proton conductivities are still too low for fuel cell applications. It is believed that this disadvantage may be overcome by using phase separated multiblock copolymers instead of random copolymers. It was reported that ion containing block copolymers with phase-separated microstructures have a better performance than random terpolymers at low hydration levels. This behaviour corresponds to the formation of a co-continuous hydrophilic-hydrophobic morphology [57, 65, 66].

However, since under certain conditions a small angle x-ray reflection has been observed in the sPPSO2PO terpolymers, the details of their morphology needs careful investigations.

The mechanical properties of sulfonated poly(phenylene sulfone)s have considerably been improved by means of terpolymerization with triphenylphosphine oxide moieties. Even under high humidification the terpolymers form clear, flexible membranes the stress at break of which in some cases exceeds that of Nafion® under the same conditions by 40%.

Acknowledgments

The authors thank S. Seywald and P. Raeder for assistance in obtaining GPC and thermal analysis data, A. Hanewald for assistance with the tensile tests and H. Burg for obtaining AFM images. Furthermore the authors acknowledge the financial support by the BMBF/Germany (03SF0323D).

References

[1] B. C. H: Steele, A. Heinzel, *Nature* **2001**, *414*, 345.

[2] M. A. Hickner, H. Ghassemi,Y. S. Kim, B. R. Einsla, J. E. McGrath, *Chem. Rev.* **2004,** *104*, 4587.

[3] J. A. Kerres, *Fuel Cells* **2005**, *5*, 230.

[4] K. D. Kreuer, *J. Membr. Sci.* **2001**, *185*, 29.

[5] W. L. Harrison, M. A. Hickner, Y. S. Kim, E. McGrath, *Fuel cells* **2005**, *5*, 2001.

[6] R. Souzy, B. Ameduri, *Prog. Polym. Sci.* **2005**, *30*, 644.

[7] J. Roziere, D. J. Jones, *Annu. Rev. Mater. Res.* **2003**, *33*, 503.

[8] J. A. Kerres, *J. Membr. Sci.* **2001**, *185*, 3.

[9] Q. Li, R. He, J.O. Jensen, N.J. Bjerrum, *Chem. Mater.* **2003**, *15*, 4896.

[10] M. Rikukawa, K. Sanui, *Prog. Polym. Sci.* **2000**, *25*, 1463.

[11] K. D. Kreuer, S. J. Paddison, E. Spohr, M. Schuster, *Chem. Rev.* **2004**, *104*, 4637.

[12] M. Schuster, K. D. Kreuer, H. T. Andersen, J. Maier, *Macromolecules* **2007**, *40*, 598.

[13] K. B. Wiles, V. A. Bhanu, F. Wang, M. A. Hickner, J. E. McGrath, *Polym. Prepr.* **2003**, *44*, 1089.

[14] Z. Bai, M. Yoonessi, S. B. Juhl, L. F. Drummy, M. F. Durstock, T. D. Dang, *Macromolecules* **2008**, *41*, 9483.

[15] D. S. Phu, Ch. H. Lee, Ch. H. Park, S. Y. Lee, Y. M. Lee, *Macromol. Rapid Commun.* **2009**, *30*, 64.

[16] J. Kerres, A. Ullrich, F. Meier, Th. Haring, *Solid State Ionics* **1999**, *125*, 243.

[17] M. Gil, X. Ji, X. Li, H. Na, J. Eric Hampsey, Y. Lu, *J. Membr. Sci.* **2004**, *234*, 75.

[18] P. Xing, G.P. Robertson, M.D. Guiver, S.D. Mikhailenko, K. Wang, S. Kaliaguine, *J. Membr. Sci.* **2004**, *229*, 95.

[19] X. Yue, M. Zhu, H. Zhang, B. Liu, Y. Wang, Z. Jiang, *J. Polym. Sci.,Part A: Polym. Chem.* **2008**, *46*, 7002.

[20] B. Liua, Y. S. Kimb,W. Huc, G. P. Robertson, B. S. Pivovar, M. D. Guiver, *J. Power Sources* **2008**, *185*, 899.

[21] Y. S. Kim, M. A. Hickner, L. Dong, B.S. Pivovar, J. E. McGrath, *J. Membr. Sci.* **2004**, *243*, 317.

[22] W. L. Harrison, M. A. Hickner, Y. S. Kim, J. E. McGrath, *Fuel Cells* **2005**, *5*, 201.

[23] H. Ghassemi, G. Ndip, J. E. McGrath, *Polymer* **2004**, *45*, 5855.

[24] K.-S. Lee, M.-H. Jeong, J.-P. Lee, J.-S. Lee, *Macromolecules* **2009**, *42*, 584.

[25] K. Matsumoto, T. Higashihara, M. Ueda, *Macromolecules* **2009**, *42*, 1161.

[26] K. Miyatake, H. Zhou, T. Matsuo, H. Uchida, M.Watanabe, *Macromolecules* **2004**, *37*, 4961.

[27] K. Chen, X. Chen, K. Yaguchi, N. Endo, M. Higa, K. Okamoto, *Polymer* **2009**, *50*, 510.

[28] Y. Yin, O. Yamada, Y. Suto, T. Mishima, K. Tanaka, H. Kita, K. Okamoto, *J. Polym. Sci., Part A: Polym. Chem.* **2005**, *43*, 1545.

[29] T. Yasuda, Y. Li, K. Miyatake, M. Hirai, M. Nanasawa, M. Watanabe, *J. Polym. Sci., Part A: Polym. Chem.* **2006**, *44*, 3995.

[30] J. Mader, L. Xiao, T. J. Schmidt, B. C. Benicewicz, *Adv. Polym. Sci.* **2008**, *216*, 63.

[31] P. Mustarelli, E. Quartarone, S. Grandi, A. Carollo, A. Magistris, *Adv. Mater.* **2008**, *20*, 1339.

[32] X. Glipa, M. El Haddad, D. J. Jones, J. Roziere, *Solid State Ionics* **1997**, *97*, 323.

[33] M. B. Gieselman, J. R. Reynolds, *Macromolecules* **1992**, *25*, 4832.

[34] P. Jannasch, *Fuel Cells* **2005**, *5*, 248.

[35] G. Alberti, M. Casciola, L. Massinelli, B. Bauer, *J. Membr. Sci.* **2001**, *185*, 73.

[36] F. Wang, M. Hickner, Y. S. Kim, T. A. Zawodzinski, J. E. McGrath, *J. Membr. Sci.* **2002**, *197*, 231.

[37] Y. Gao, G. P. Robertson, M. D. Guiver, S. D. Mikhailenko, X. Li, S. Kaliaguine, *Macromolecules* **2005**, *38*, 3237.

[38] C. Iojoiu, M. Marechal, F. Chabert, J.-Y. Sanchez, *Fuel Cells* **2005**, *5*, 344.

[39] J. A. Kerres, W. Cui, S. Reichle, *J. Polym. Sci., Part A: Polym. Chem.* **1996**, *34*, 2421.

[40] J. A. Kerres, W. Zhang, W. Cui, *J. Polym. Sci., Part A: Polym. Chem.* **1998**, *36*, 1441.

[41] M. Ueda, H. Toyota, T. Ouchi, J.-I Sugiyama, K. Yonetake, T. Masuko, T. Teramoto, *J. Polym. Sci., Part A: Polym. Chem.* **1993**, *31*, 853.

[42] W. L. Harrison, F. Wang, J. B. Mecham, V. A. Bhanu, M. Hill, Y. S. Kim, J. E. McGrath, *J. Polym. Sci., Part A: Polym. Chem.* **2003**, *41*, 2264.

[43] X. Mua, C. Zhang, G. Xiao, D. Yan, G. Sun, *J. Polym. Sci., Part A: Polym. Chem.* **2008**, *46*, 1758.

[44] X. Ma, L. Sheng, C. Zhang, G. Xiao, D. Yan, G. Sun, *J. Membr. Sci.* **2008**, *310*, 303.

[45] C. Zhang, S. Kang, X. Ma, G. Xiao, D. Yan, *J. Membr. Sci.* **2009**, *329*, 99.

[46] D. J. Riley, A. Gungor, S. A. Srinivasan, M. Sankarapandian, C. Tchatchoua, M. W. Muggli, T. C. Ward, J. E. McGrath, *Polym. Eng. Sci.* **1997**, *37*, 1501.

[47] S. Wang, Q. Ji, C. N. Tchatchoua, A. R. Shultz, J. E. McGrath, *J. Polym. Sci., Part B: Polym. Phys.* **1999**, *37*, 1849.

[48] S. Wang, H. Zhuang, H. K. Shobha, T. E. Glass, M. Sankarapandian, Q. Ji, A. R. Shultz, J. E. McGrath, *Macromolecules* **2001**, *34*, 8051.

[49] L. Greenspan, *J. Res. Nat. Bur. Stand. A* **1977**, *81*, 89.

[50] D. Xing, J. A. Kerres, *Polym. Adv. Technol.* **2006**, *17*, 591.

[51] L. Holliday, in *Ionic Polymers* (Ed: L. Holliday), Applied Science, London **1975**.

[52] T. A. Zawodzinski, T. E. Springer, J. Davey, R. Jestel, C. Lopez, J. Valerio, S. Gottesfeld, *J. Electrochem. Soc.* **1993**, *140*, 1981.

[53] P. V. Schroeder, *Z. Phys. Chem.* **1903**, *45*, 75.

[54] P. Choi, R. Datta, *J. Electrochem. Soc.* **2003**, *150*, E601.

[55] V. Freger, *J. Phys. Chem. B* **2009**, *113*, 24.

[56] C. Vallieres, D. Winkelmann, D. Roizard, E. Favre, P. Scharfer, M. Kind, *J. Membr. Sci.* **2006**, *278*, 357.

[57] G. Alberti, R. Narducci, M. Sganappa, *J. Power Sources* **2008**, *178*, 575.

[58] M. L. Di Vona, E. Sgreccia, S. Licoccia, G. Alberti, L. Tortet, P. Knauth, *J. Phys. Chem. B* **2009**, *113,* 7505.

[59] A. Roy, H.-S. Lee, J. E. McGrath, *Polymer* **2008**, *49*, 5037.

[60] K. D. Kreuer, *Solid State Ionics* **2000**;*136–137*,149.

[61] T. E. Springer, T. A. Zavodzinski, S. Gottesfeld, *J. Electrochem. Soc.* **1991**, *138*, 2334.

[62] B. J. Alder, J. H. Hildebrand, *Ind. Eng. Chem. Fundam.,* **1973**, *12*, 387.

[63] C. C. de Araujo, K. D. Kreuer, M. Schuster, G. Portale, H. Mendil-Jakani, G. Gebel, J. Maier, *Physical Chemistry Chemical Physics* **2009**, *11*, 3305.

[64] U. Beuschern, S. J. C. Cleghorn, W. B. Johnson, *Int. J. Energy Res.* **2005**, *29*, 1103.

[65] A. Roy, M.A. Hickner, X. Yu, Y. Li, T.E. Glass, J. E. McGrath, J. Polym. Sci., Part B: Polym. Phys. **2006**, *44*, 2226.

[66] H. Ghassemi, J. E. McGrath, J. T. A. Zawodzinski, *Polymer* **2006**, *47*, 4132.

Tables

Table 1 Polymer analytical data of the synthesized terpolymers

polymers	K : L : M : N (k : l : m : n)	IEC mequiv g^{-1} (theor)	M_n, g mol^{-1}	M_w, g mol^{-1}	D	T_{d5}, °C
sPPSO2PO-1	4:2:1:7	1,74	37.174	96.990	2,61	315
sPPSO2PO-2	4:1:2:7	1,72	46.074	159.510	3,46	315
sPPSO2PO-3	7:1:2:10	2,01	32.585	79.677	2,45	310
sPPSO2PO-4	6:1:1:8	2,19	42.597	116.577	2,74	320
sPPSO2PO-5	6:1:1:8	2,32	70.461	128.729	1,82	340

k,l.m,n are molar ratios of the monomers K,L,M,N (see Scheme.1)

Table 2 Water uptake, shrinkage and mechanical properties for obtained sPPSO2PO terpolymers.

polymers	λ*	λ**	$\Delta d_{52.4\%}$ $\Delta l_{52.4\%}$	$\Delta d_{34\%}$ $\Delta l_{34\%}$	$\Delta d_{20\%}$ $\Delta l_{20\%}$	Stress at break (MPa)		Elongation at break (%)		Young's modulus (MPa)	
						50%	100%	50%	100%	50%	100%
sPPSO2PO-1	-	22.0	-	-	-	-	-	-	-	-	
sPPSO2PO-2	13.3	24.1	-	-	-	-	-	-	-	-	-
sPPSO2PO-3	12.7	25.6	-21 -11	-21 -11	-21 -11	14.3	-	15.0	-	661.4	-
sPPSO2PO-4	12.8	28.1	-23 -12	-23 -12	-23 -12	16.6	-	18.7	-	781.9	-
sPPSO2PO-5	12.6	19.3	-25 -13	-23 -13	-24 -15	21.6	10.9	19.8	37.7	839.9	156.4
Nafion 117	12.8	20.5	-6 -12	-6 -13	-7 -13	13.4	-	191.1	-	150.4	-

* λ: number of water molecules per sulfonic acid measured under saturated water vapor.

** λ: number of water molecules per sulfonic acid measured by direct contact with water.

Δd and Δl present the change in thickness and length of films stored at the specified RH.

Figure Captions

Fig. 1. ^{1}H NMR of sPPSPO-3 and its corresponding oxidized form sPPSO2PO-3.

Fig. 2. TGA curves for sPPSO2PO terpolymers

Fig. 3. Water uptake of sPSO2PO membranes under different relative humidity.

Fig. 4. Proton conductivities of sPPSO2PO terpolymers as a function of RH.

* through plane measurements

Fig. 5. Proton conductivity data at 95% RH as a function of IEC.

Fig. 6. Proton conductivity versus temperature at 80% RH.

Fig. 7. Proton conductivity of sPSSO2PO-2, sPSSO2PO-4 and sPSSO2PO-5 as a function of temperature measured under 1 bar water vapor pressure.

Fig. 8. The weight losses of different PSO2PO membranes in Fenton's reagent.

Fig. 9. Stress versus strain curves for membranes sPPSO2PO-3, sPPSO2PO-4 and sPPSO2PO-5 at 50% RH and 25°C, and for sPPSO2PO-5 at 100% RH and 25°C, compared to the Nafion® 117 data and sPPSO2-X.

Scheme Caption

Scheme 1. Synthesis of sPPSO2POs

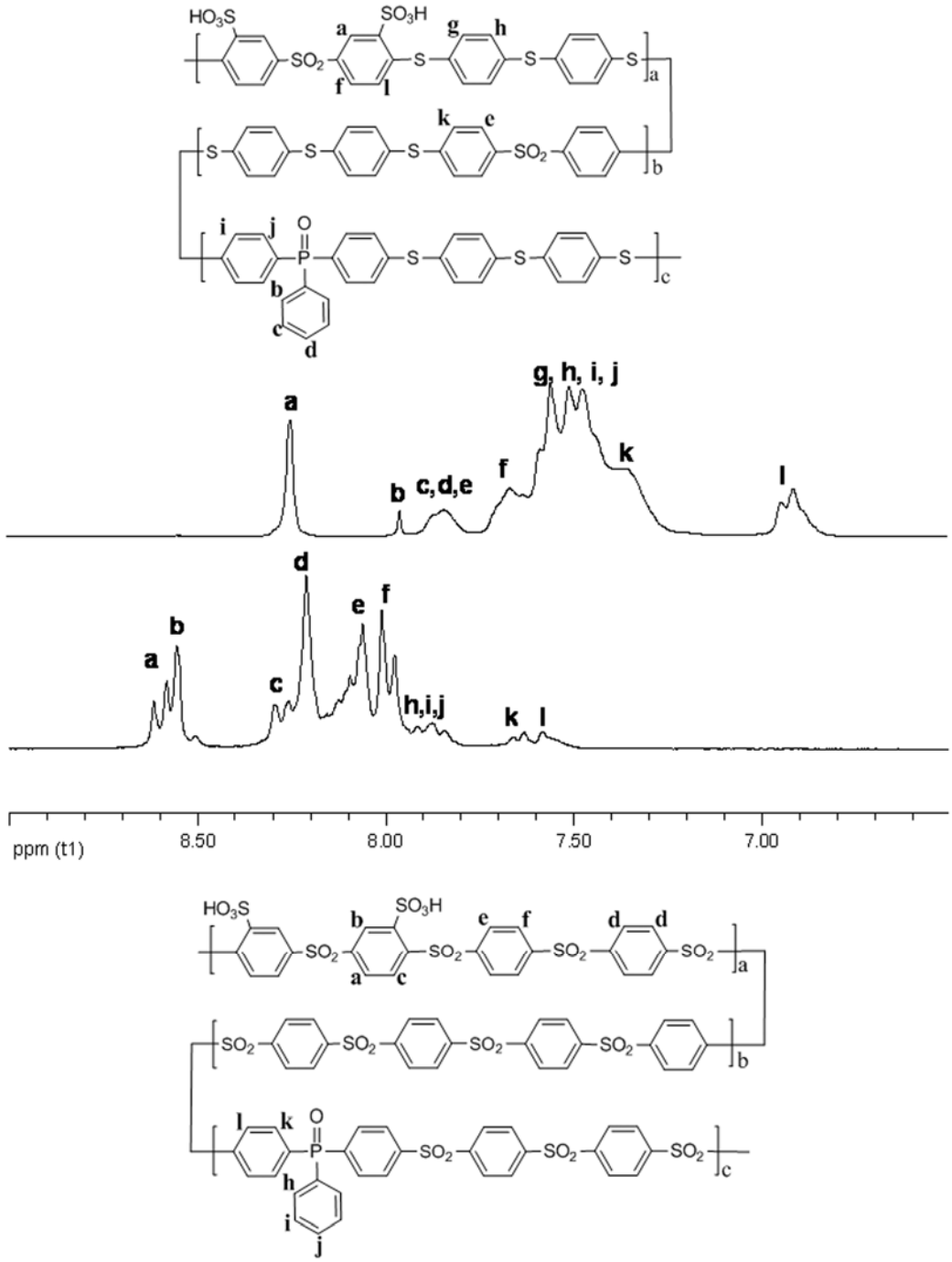
HO3S
SO3H
SO2
S
a
b
c
d
e
f
g
h
i
j
k
l
g, h, i, j
c,d,e
h,i,j
ppm (t1)
8.50
8.00
7.50
7.00

Figure 1

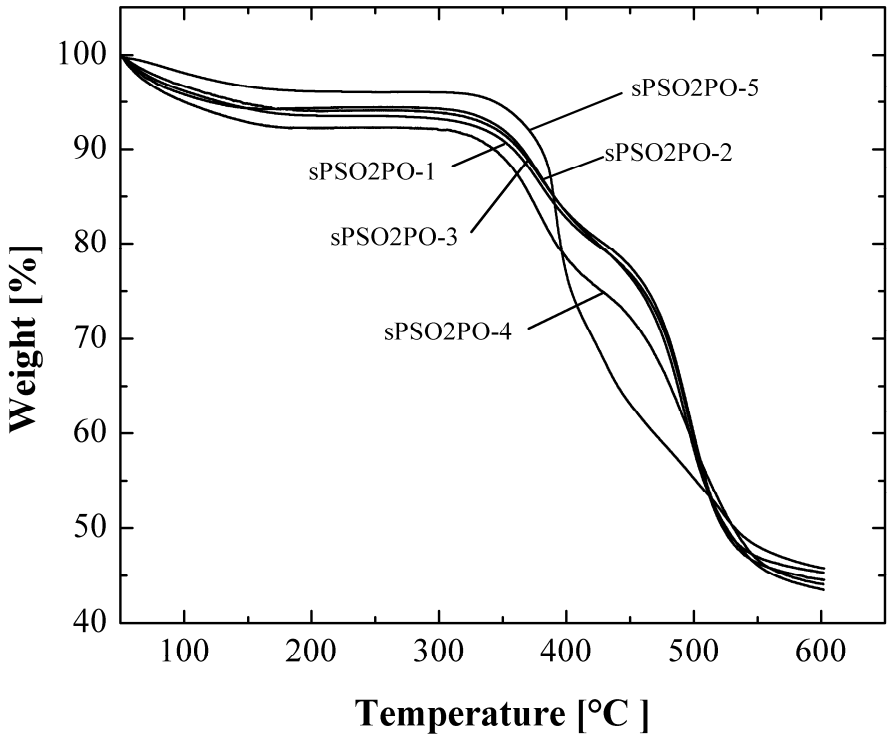

Figure 2

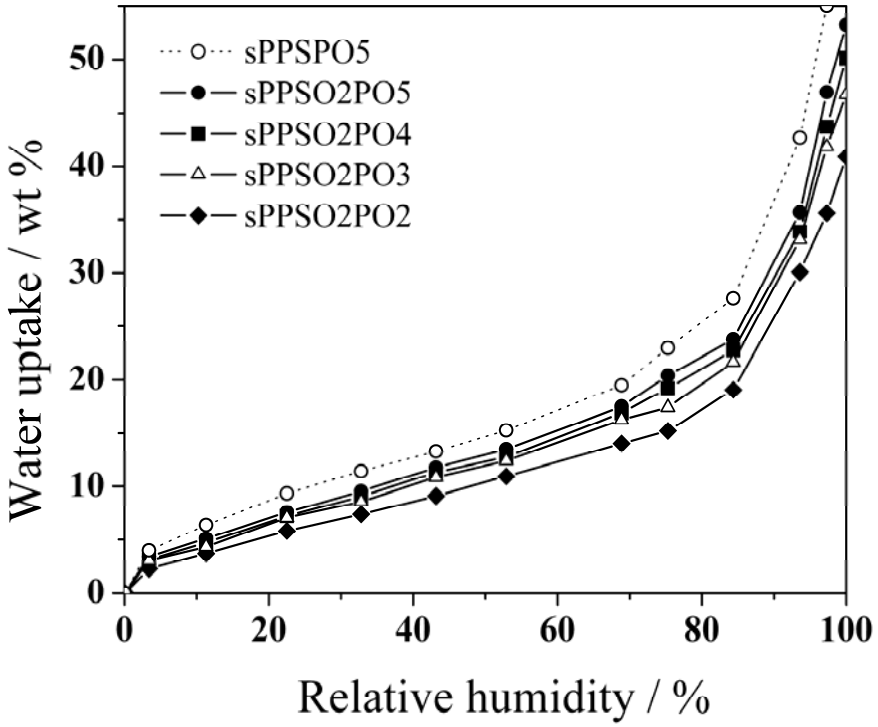

Figure 3

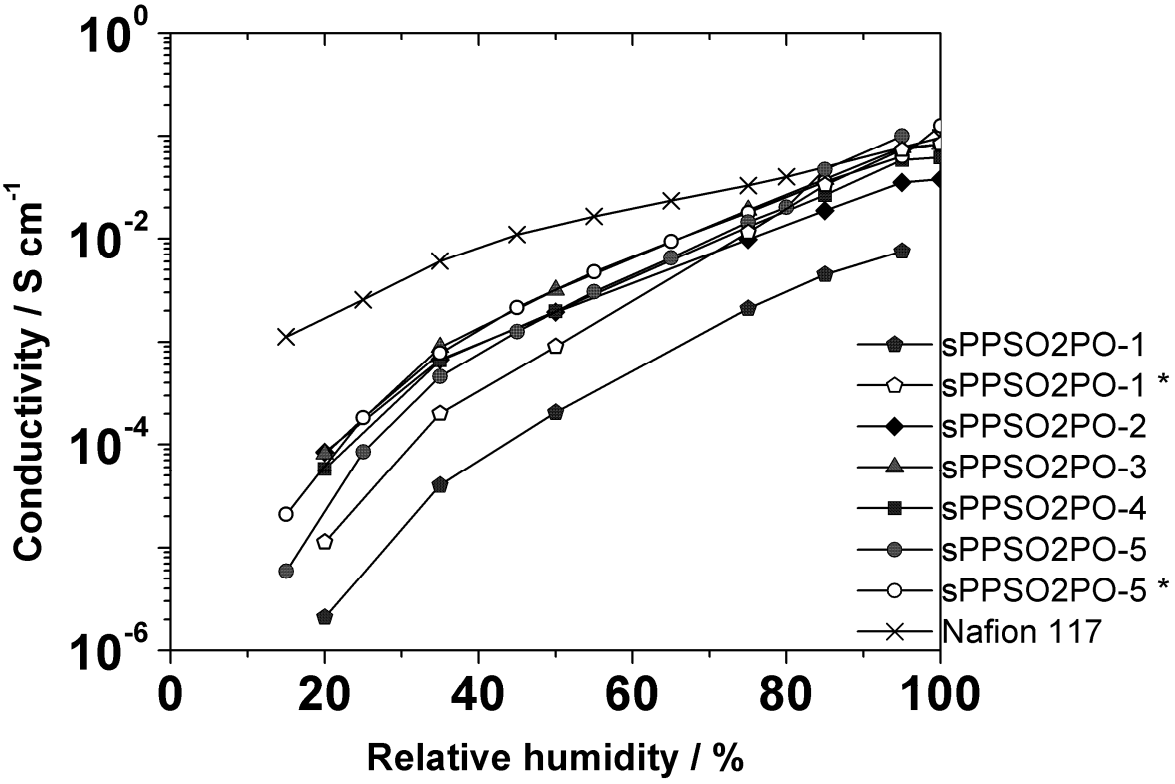

Figure 4

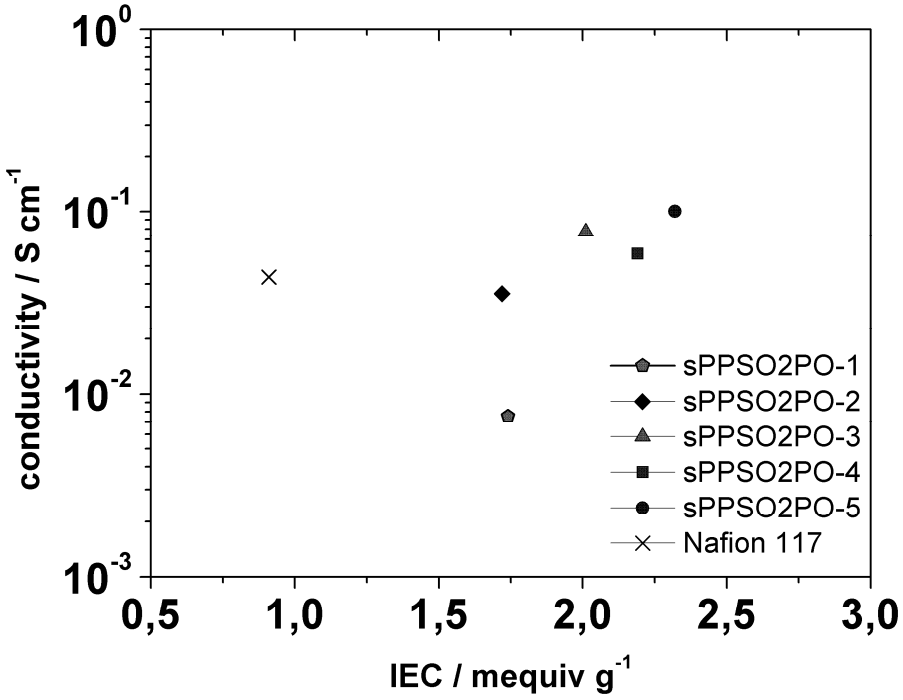

Figure 5

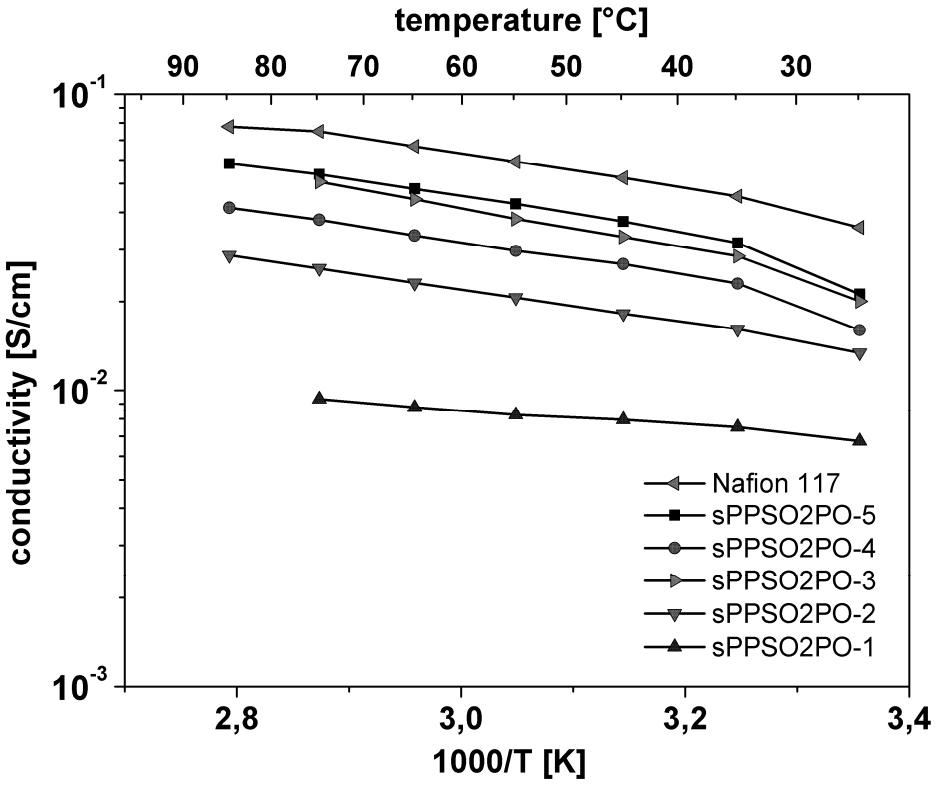

Figure 6

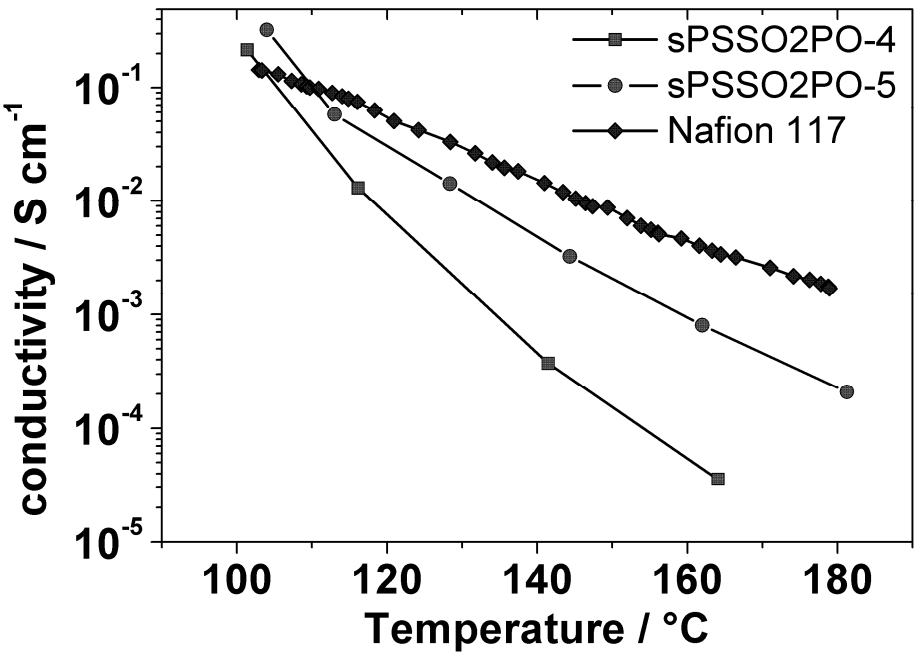

Figure 7

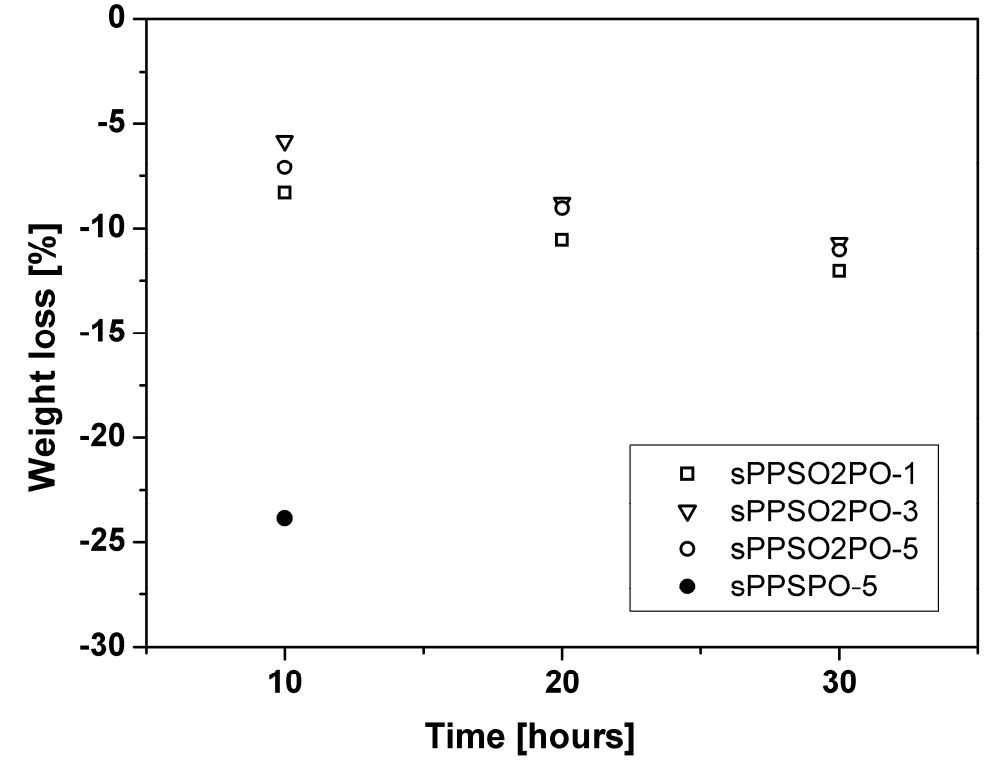

Figure 8

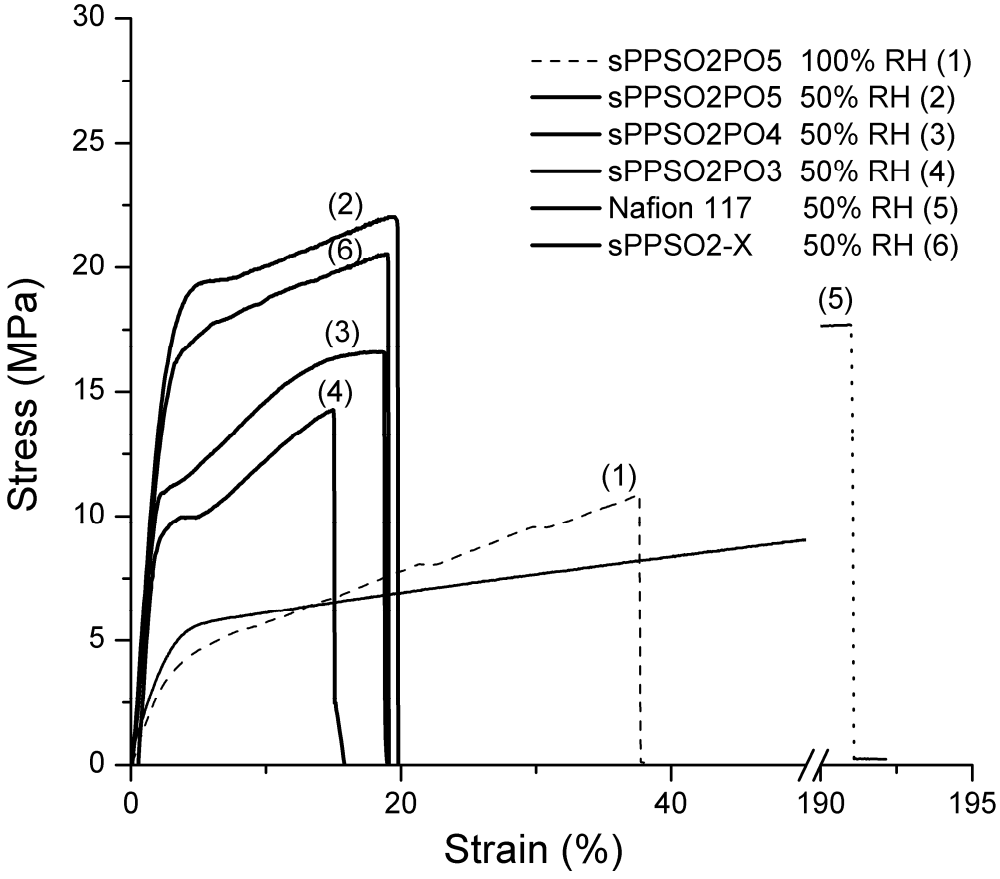

Figure 9

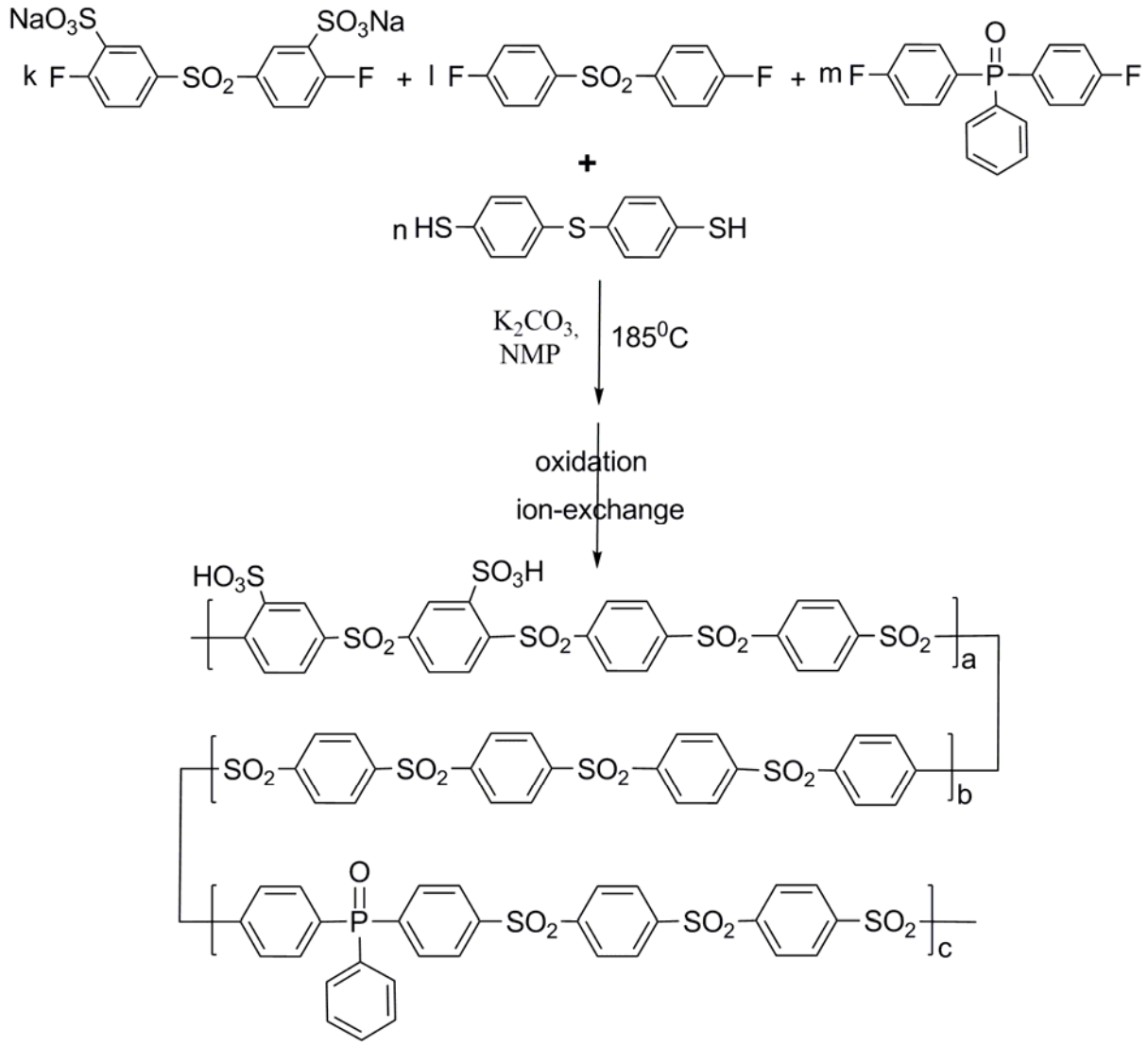
NaO3S
SO3Na
k F
SO2
F
+ l F
SO2
F
+ m F
O
P
F
+
n HS
S
SH
K2CO3,
NMP
185⁰C
oxidation
ion-exchange
HO3S
SO3H
SO2
a
b
c

Scheme 1